# Supporting Information

## Artificial Solid-Electrolyte Interphase Enabling One-Step Sulfur Transition in Polyethylene Oxide-Based Solid-State Lithium-Sulfur Batteries

Leicheng Zhang[a,1], Tianshuai Wang[a,1], Junjie Chen [a,1], Maochun Wu[c,*], Tianshou Zhao[a,b,*]

[a] Department of Mechanical and Aerospace Engineering, The Hong Kong University of Science and Technology, Clear Water Bay, Kowloon, Hong Kong SAR, China

[b] Department of Mechanical and Energy Engineering, Southern University of Science and Technology, Shenzhen, 518055, China

[c] Department of Mechanical Engineering, The Hong Kong Polytechnic University, Hung Hom, Kowloon, Hong Kong SAR, China

[1] These authors contributed equally to this work.

* Corresponding authors:

E-mail: maochun.wu@polyu.edu.hk (M.C. Wu)

E-mail: metzhao@ust.hk, zhaots@sustech.edu.cn (T.S. Zhao)

**Material characterizations**

The morphology of samples was observed by scanning electron microscopy (SEM) conducted on a JOEL-6700 SEM instrument at an accelerating voltage of 10 kV. X-ray photoelectron spectroscopy (XPS) was conducted on a Physical Electronics PHI 5600 multi-technique system using an Al monochromatic X-ray source at 350 W.

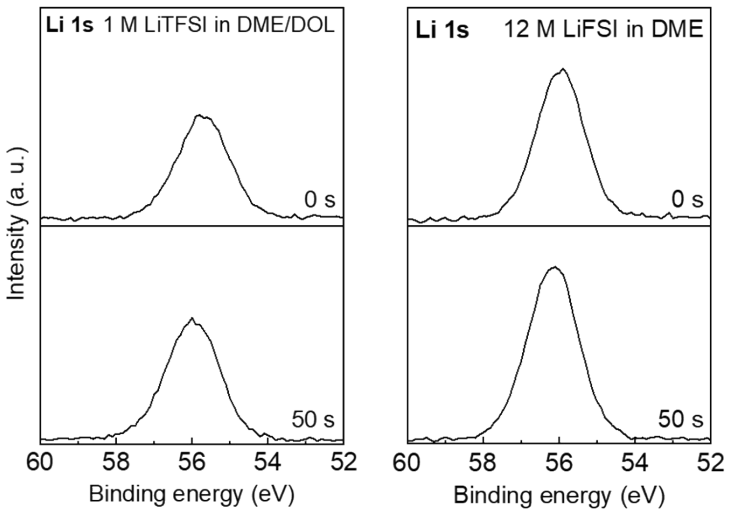


**Fig. S1.** Li 1s spectra on S cathodes using different electrolytes.

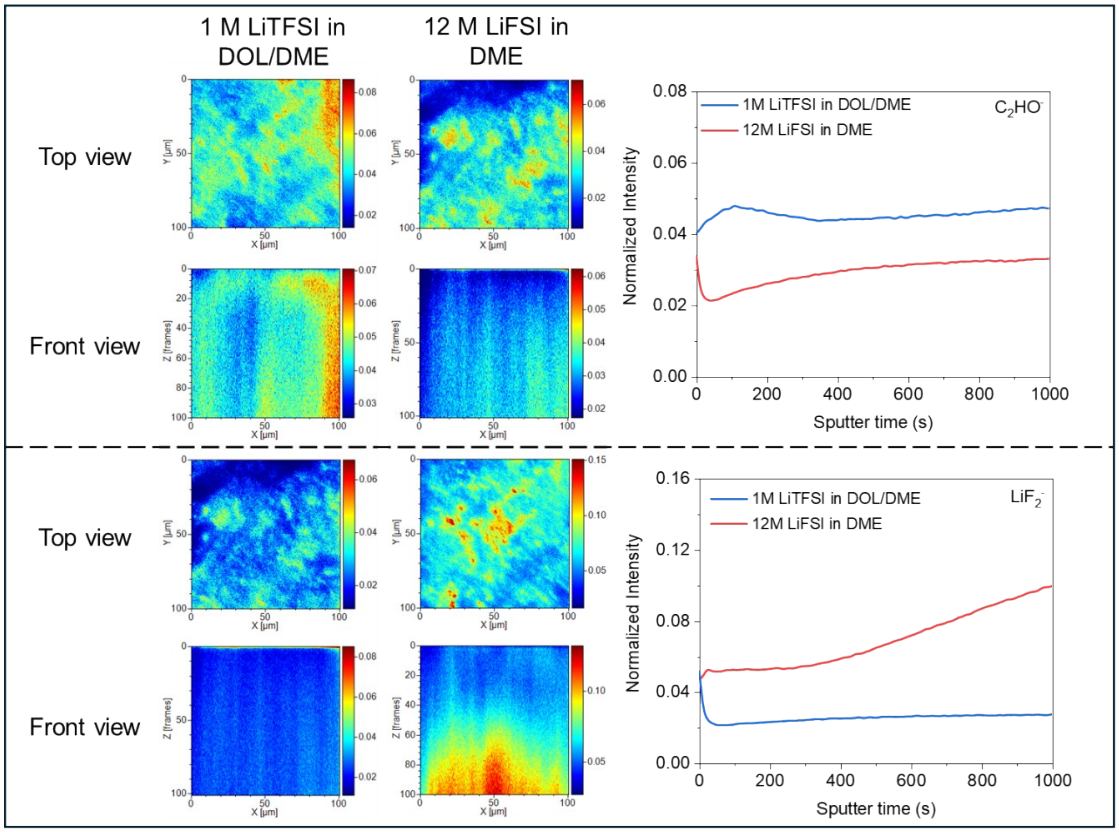


**Fig. S2**. TOF-SIMS results of CEI from

1 M LiTFSI in DOL/DME and 12 M LiFSI in DME.

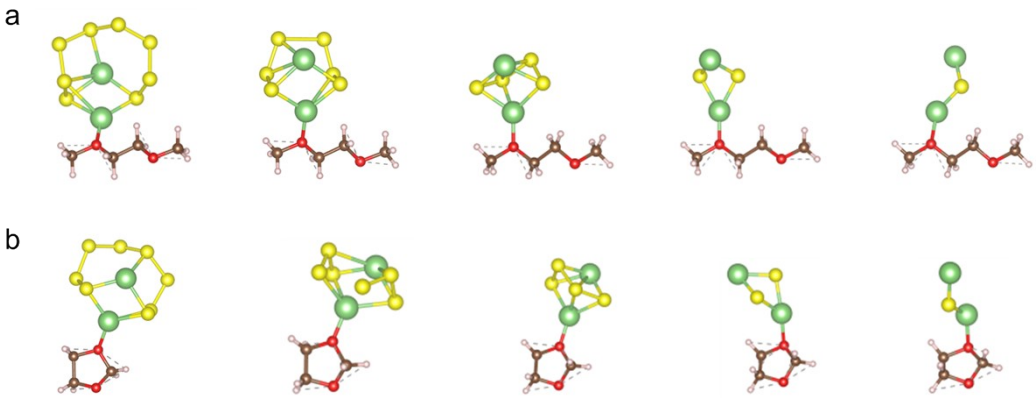


**Fig. S3.** The relaxed binding configurations of single (a) DME and (b) DOL with $Li_2S_n$ (n = 8, 6, 4, 2, 1).

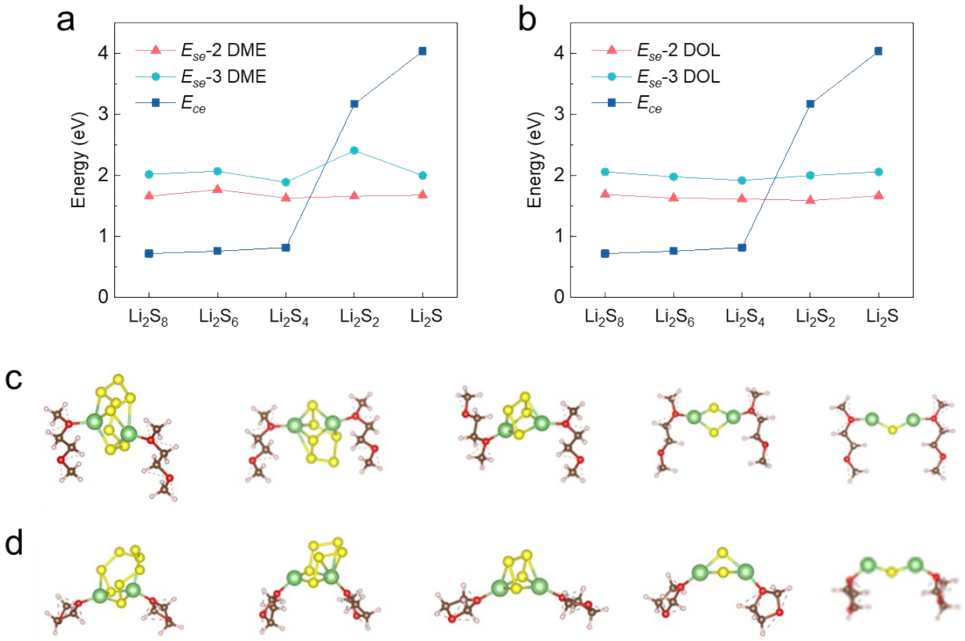


**Fig. S4.** $E_{ce}$ of $Li_2S_n$ and their $E_{se}$ with double and triple (a) DME and (b) DOL molecules. The relaxed binding configurations of $Li_2S_n$ with double (c) DME and (d) DOL. (n = 8, 6, 4, 2, 1)

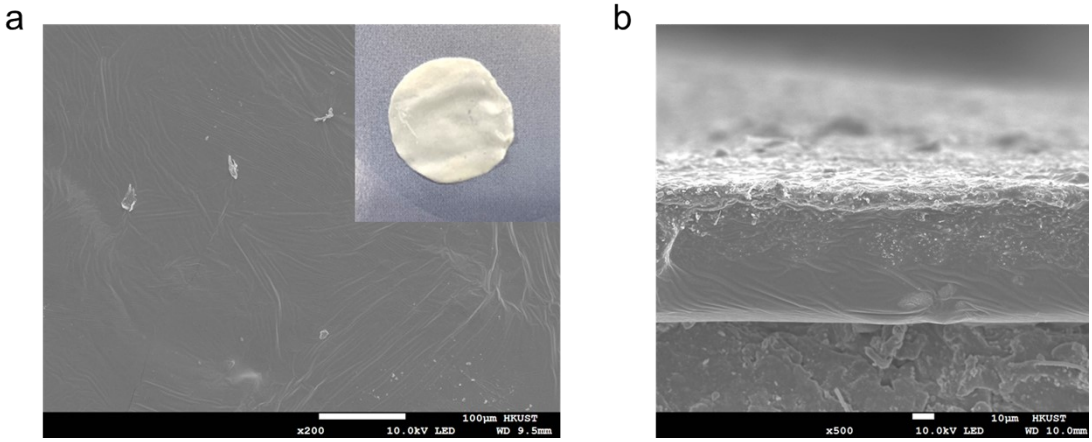


**Fig. S5.** SEM images of PPG from (a) top-view (Inset: digital photo of PPG) and (b) side-view.

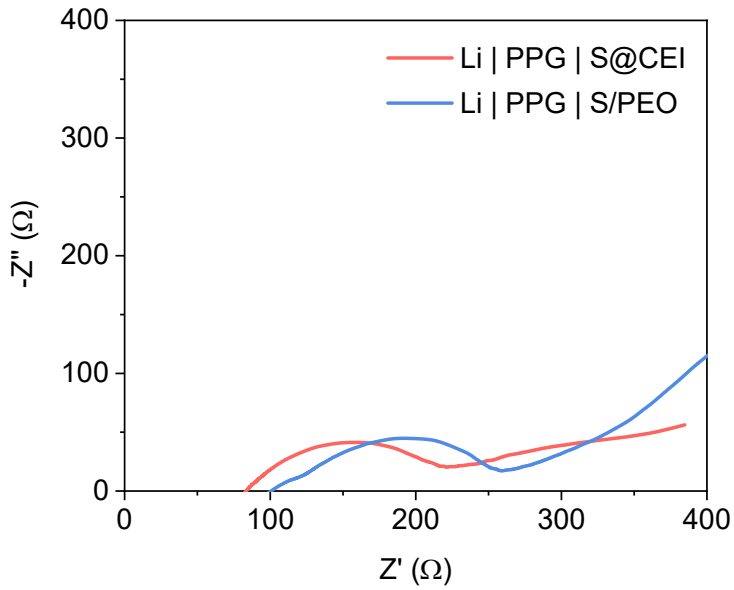


**Fig.S6**. EIS plots of two cells with S/PEO and S@CEI cathodes.

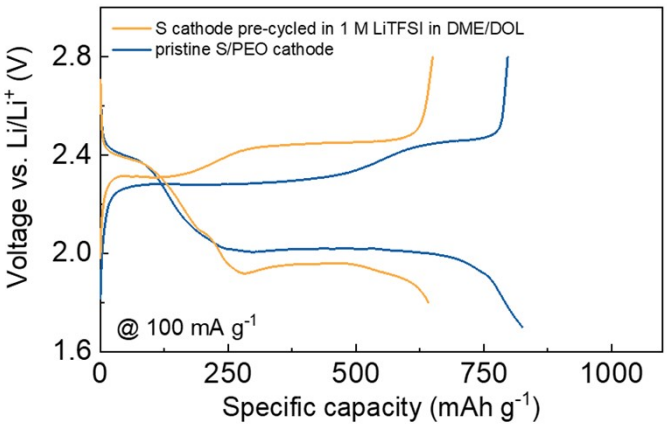


**Fig. S7.** Voltage profiles of Li | PPG | S/PEO, and Li | PPG | S cathode pre-cycled in 1 M LiTFSI in DME/DOL.

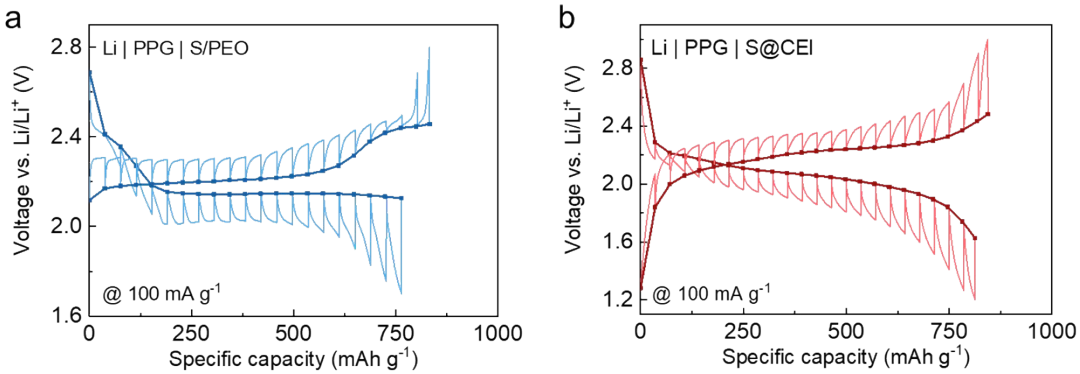


**Fig. S8.** GITT curves of (a) Li | PPG | S/PEO cell and (b) Li | PPG | S@CEI cell.

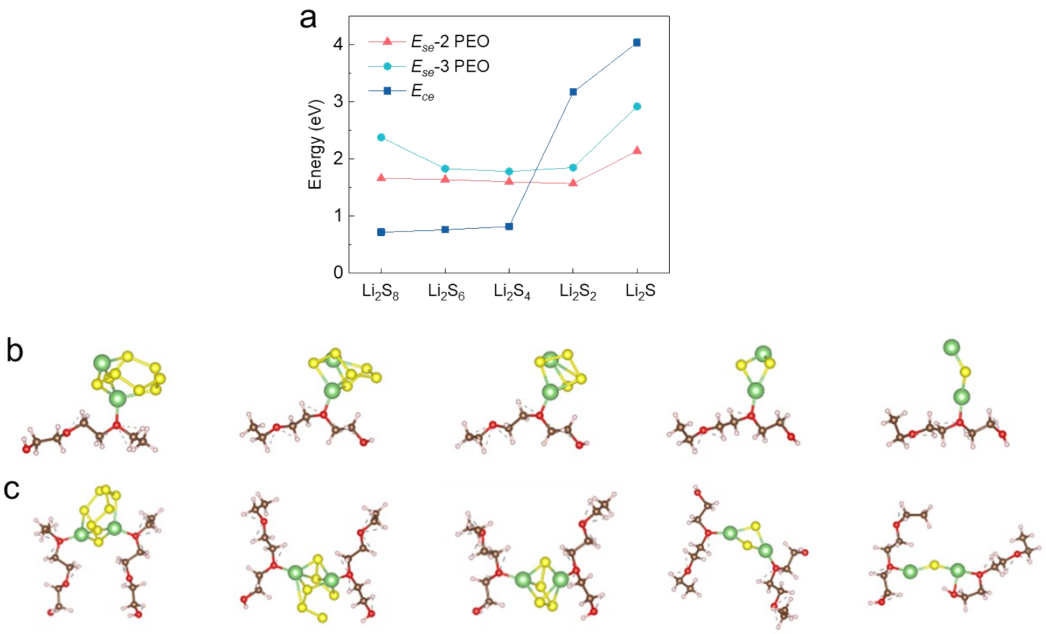


**Fig. S9.** (a) $E_{ce}$ of $Li_2S_n$ and their $E_{se}$ with double and triple Li-O bonds of PEO. The relaxed binding configurations of $Li_2S_n$ with (b) single and (c) double Li-O bonds. (n = 8, 6, 4, 2, 1)

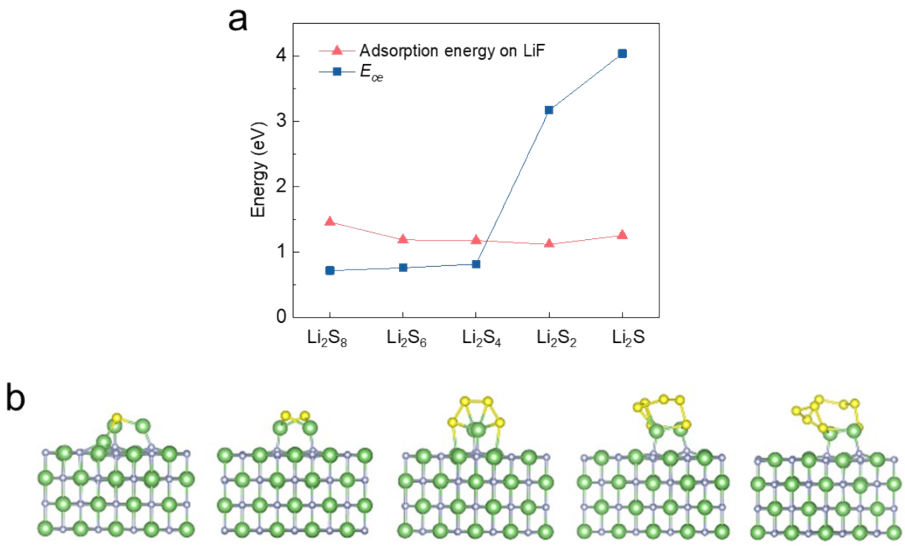


**Fig. S10.** (a) Comparison between $E_{ce}$ of polysulfides and their adsorption energies on the (001) surface of LiF. (b) The relaxed binding configurations of $Li_2S_n$ (n = 1, 2, 4, 6, 8) on the (001) surface of LiF.

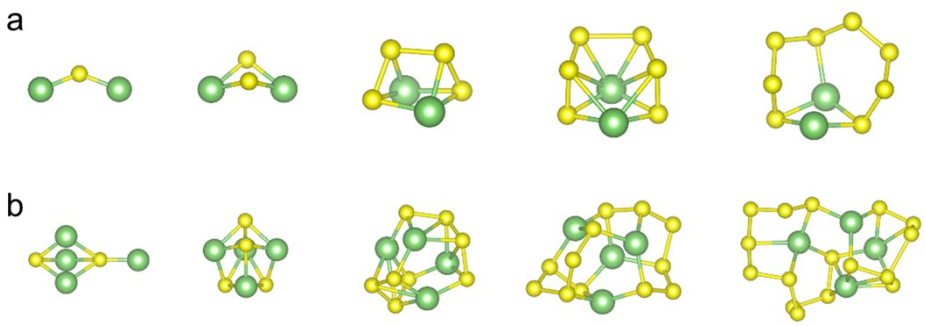


**Fig. S11.** (a) Monomer phase and (b) dimer phase molecule configurations of $Li_2S_n$ (n = 1, 2, 4, 6, 8).

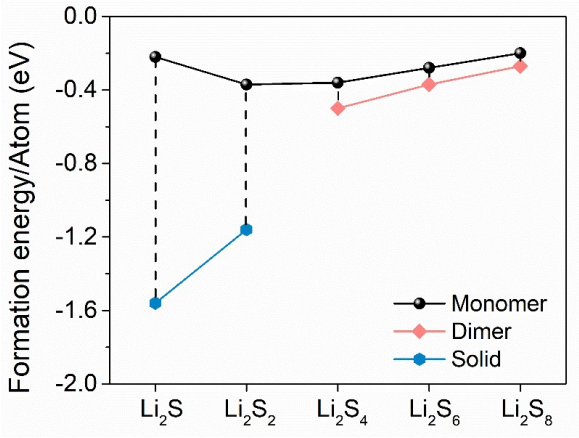


**Fig. S12.** The formation energy of the monomer, dimer, and solid phase of $Li_2S_n$ (n = 1, 2, 4, 6, 8).

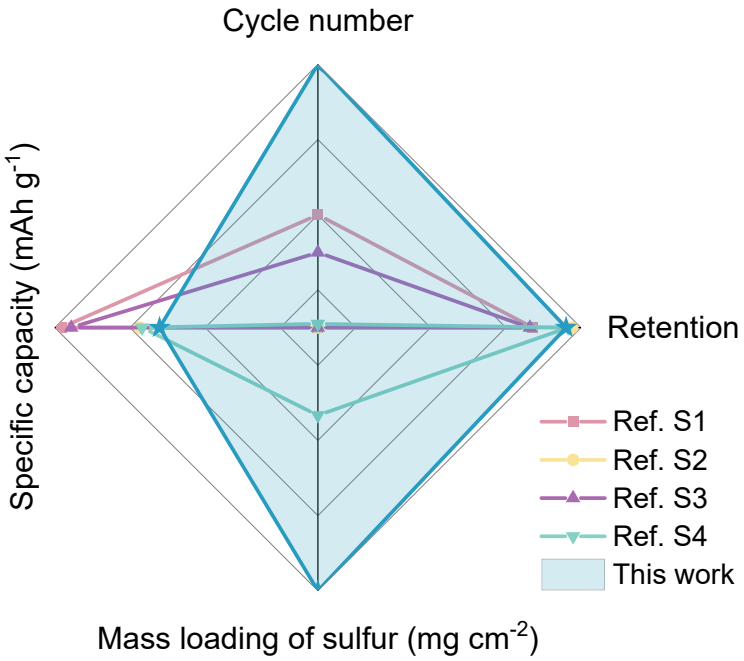


**Fig. S13.** Performance comparisons of solid-state Li–S batteries between this work and related reports.

We have compared our work with the relevant literature reported. This work demonstrates prominent performance in terms of cycle number, retention, mass loading of sulfur, and specific capacity, highlighting the significant contribution of constructing a CEI for long-term battery cycling (Ref. S1: *J. Am. Chem. Soc.* 2021, **143**, 43, 18188–18195; Ref. S2: *J. Mater. Chem. A*, 2023, **11**, 19046-19055; Ref. S3: *J. Mater. Chem. A*, 2020, **8**, 16451-16462; Ref. S4: *Chem. - A Eur. J.* 2017, **23** (56), 13950–13956).

**Table S1**. Performance comparisons between this work and other related reports.

| | **Cycle number** | **Retention** | **Mass loading of S (mg cm$^{-2}$)** | **Specific capacity (mAh g$^{-1}$)** |
|---|---|---|---|---|
| Ref. S1 *(J. Am. Chem. Soc.* 2021, **143**, 43, 18188–18195) | 120 | 45.2% | 0.5 | 1415 |
| Ref. S2 *(J. Mater. Chem. A*, 2023, **11**, 19046-19055) | 60 | 90% | 0.5 | 982 |
| Ref. S3 *(J. Mater. Chem. A*, 2020, **8**, 16451-16462) | 100 | 41.9% | 0.5 | 1360 |
| Ref. S4 *Chem. – A Eur. J.* 2017, **23** (56), 13950–13956 | 62 | 85.3% | 0.6 | 969 |
| This work | 200 | 83.1% | 0.8 | 873 |